

Supplementary information for

High-efficiency and stable photoluminescence of  $\text{CH}_3\text{NH}_3\text{PbBr}_3@ \text{CsPbBr}_3$   
perovskite quantum dot

Yajing Wang,<sup>a,b</sup> Ahui Li,<sup>a,b</sup> Yizhen Hu,<sup>a,b</sup> Yanping Bao,<sup>a,b</sup> Yongfan Zhang,<sup>a</sup> Xiaolin  
Hu,<sup>\*a,b</sup> and Naifeng Zhuang<sup>a,b</sup>

<sup>a</sup> College of Chemistry, Fuzhou University, Fuzhou 350108, China.

<sup>b</sup> Institute of Optical Crystalline Materials, Fuzhou University, Fuzhou 350108, China.

Email: linamethyst@fzu.edu.cn ( X. Hu)

### 1. Element composition of QDs

The scanning electron microscope (SEM) image, the X-ray energy dispersive spectroscopy (EDS), and the element mappings were observed by HIROX SH-4000 with the accelerating voltage of 5-30 kV. The results are shown in Fig. S1. The element mappings (Fig. S1c-e) show that in addition to C, H, and N elements,  $\text{CH}_3\text{NH}_3\text{PbBr}_3@ \text{CsPbBr}_3$  QDs also contain Cs, Pb, and Br elements in a uniform distribution. For confirming the composition, EDS of QDs is adopted and shown in Fig. S1b. The atomic composition of Cs, Pb, and Br are 13.1, 21.0, and 65.9 at.%, respectively. Thus, the mole ratio of Pb:Br is about 1:3, which conforms to the stoichiometric ratio.

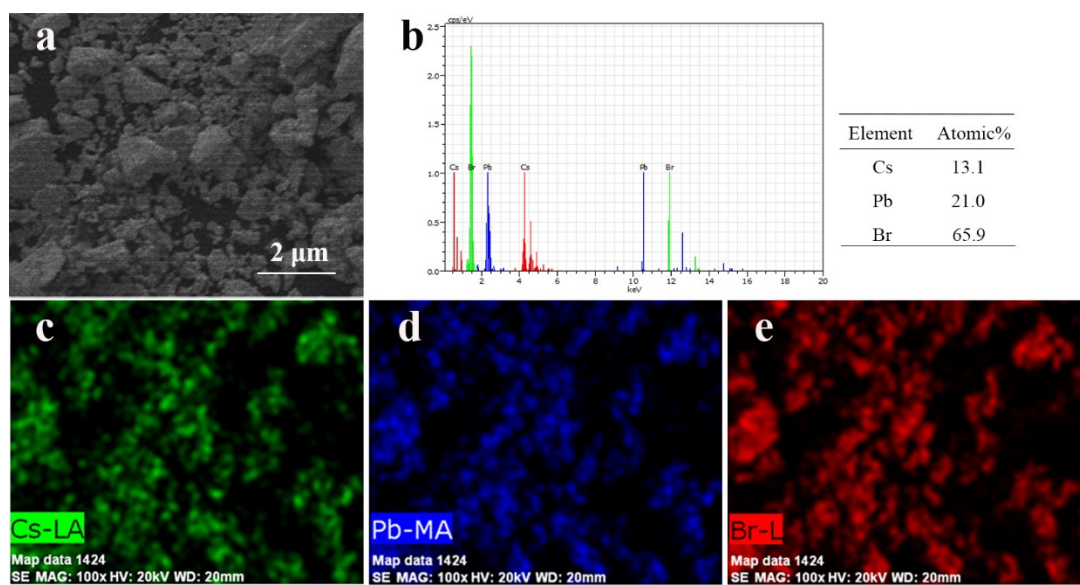


Fig. S1 SEM image (a), EDS spectroscopy (b), and element mappings (c-e) of

$\text{CH}_3\text{NH}_3\text{PbBr}_3@ \text{CsPbBr}_3$  QDs.

## 2. Crystal structure collapse

Experiencing high temperature from the electron beam radiation, the crystal structure of organic shell in  $\text{CsPbBr}_3@ \text{CH}_3\text{NH}_3\text{PbBr}_3$  composite QDs collapses and loosens, and the crystallinity is reduced as the following XRD patterns (Fig. S2), so that the size of a single quantum dot expands significantly, as shown in Fig. 1c.

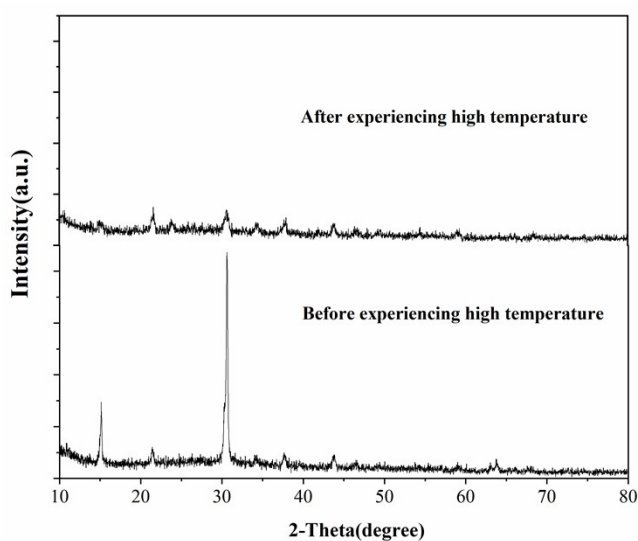


Fig. S2 XRD patterns of  $\text{CsPbBr}_3@ \text{CH}_3\text{NH}_3\text{PbBr}_3$  before and after test

### 3. XRD patterns of CH<sub>3</sub>NH<sub>3</sub>PbBr<sub>3</sub>@CsPbBr<sub>3</sub>

From the enlarged XRD patterns, as shown in the following Fig. S3, the diffraction angles of core-shell structure move to a higher value. According to the Bragg equation  $2d_{(h^*k^*l^*)} \cdot \sin \theta_{hkl} = n\lambda$ , it can be known that the smaller the interplanar spacing  $d$ , the higher the diffraction angle  $\theta$ . The unit cell parameters and the interplanar spacing  $d$  of CsPbBr<sub>3</sub> are slightly smaller than those of CH<sub>3</sub>NH<sub>3</sub>PbBr<sub>3</sub>. On the other hand, because the composite QDs include two similar crystal phases, the diffraction peaks overlap with each other and are broadened to a certain extent. Thus, compared with CH<sub>3</sub>NH<sub>3</sub>PbBr<sub>3</sub>, CH<sub>3</sub>NH<sub>3</sub>PbBr<sub>3</sub>@CsPbBr<sub>3</sub> has the higher diffraction angle and the wider full width at half maxima (FWHM) as listed in the Table S1. These observed phenomena also can confirm the core-shell structure of composite QDs.

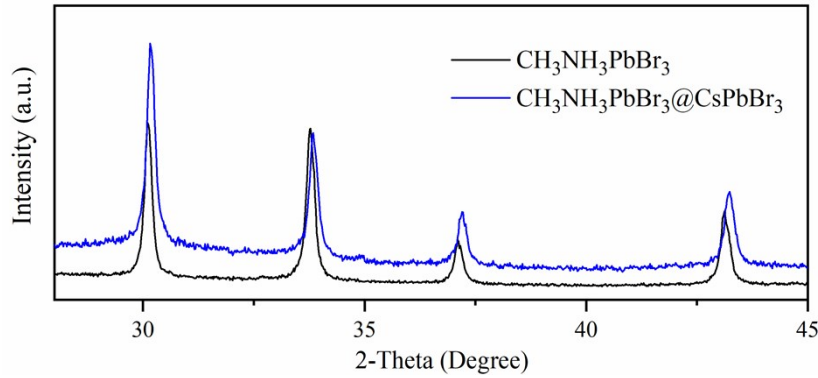


Fig. S3 XRD patterns with the diffraction angle  $2\theta$  of 28-45° for CH<sub>3</sub>NH<sub>3</sub>PbBr<sub>3</sub> and CH<sub>3</sub>NH<sub>3</sub>PbBr<sub>3</sub>@CsPbBr<sub>3</sub>

Table S1 Diffraction angle and FWHM of CH<sub>3</sub>NH<sub>3</sub>PbBr<sub>3</sub> and CH<sub>3</sub>NH<sub>3</sub>PbBr<sub>3</sub>@CsPbBr<sub>3</sub>

No.	QDs	$2\theta$ (°)	FWHM
1	CH <sub>3</sub> NH <sub>3</sub> PbBr <sub>3</sub>	30.1	0.22
	CH <sub>3</sub> NH <sub>3</sub> PbBr <sub>3</sub> @CsPbBr <sub>3</sub>	30.2	0.27
2	CH <sub>3</sub> NH <sub>3</sub> PbBr <sub>3</sub>	33.7	0.25
	CH <sub>3</sub> NH <sub>3</sub> PbBr <sub>3</sub> @CsPbBr <sub>3</sub>	33.8	0.30
3	CH <sub>3</sub> NH <sub>3</sub> PbBr <sub>3</sub>	37.1	0.30
	CH <sub>3</sub> NH <sub>3</sub> PbBr <sub>3</sub> @CsPbBr <sub>3</sub>	37.2	0.54
4	CH <sub>3</sub> NH <sub>3</sub> PbBr <sub>3</sub>	43.1	0.28
	CH <sub>3</sub> NH <sub>3</sub> PbBr <sub>3</sub> @CsPbBr <sub>3</sub>	43.3	0.39

#### 4. Theoretical calculation

In order to discuss the electric transition of PL of QDs, the partial density of states (PDOS) of  $\text{CH}_3\text{NH}_3\text{PbBr}_3$  and  $\text{CH}_3\text{NH}_3\text{PbBr}_3@\text{CsPbBr}_3$  were calculated by using the density functional theory (DFT) based on pseudopotential plane wave. (*Phys. Rev. B*, 2007, 76, 075401; *Electrochim. Acta*, 2016, 187, 560-566; *Comput. Phys. Commun.*, 1997, 107, 187; *J. Mater. Chem. C*, 2017, 5(31), 7904-7910) The pseudopotential plane wave method is suitable for periodic structure. (*Eur. Phys. J. Appl. Phys.*, 2004, 27, 251-254) All of DFT calculations were performed with Cambridge Sequential Total Energy Package (CASTEP) program package in Materials Studio software. (*Phys. Rev. B*, 2003, 68, 085327; *Z. Kristallogr.* 2005, 220(5-6), 567-570)

The (001) crystal surface of  $\text{CH}_3\text{NH}_3\text{PbBr}_3$  and  $\text{CH}_3\text{NH}_3\text{PbBr}_3@\text{CsPbBr}_3$  were cleaved based on the crystal structure of  $\text{CH}_3\text{NH}_3\text{PbBr}_3$  and  $\text{CsPbBr}_3$ , as shown in Fig. 5. The fractional thickness were 5 and then  $2 \times 2$  ( $U \times V$ ) super cells were created. The thickness of vacuum slab were built as 30 Å with the vacuum orientation of  $c$ . the geometry optimization were performed. In order to calculate accurately, the generalized gradient approximation (GGA) with Perdew-Burke-Ernzerhof (PBE) type exchange-correlation functions was adopted to treat the perovskite-type rare earth ferrite. (*Phys. Rev. Lett.*, 1996, 77, 3865; *Phys. Rev. Lett.*, 1997, 78, 1396) The plane wave basis sets are used with the ultrasoft pseudopotential. The Monkhorst-Pack grid k-points of  $2 \times 2 \times 1$ , the energy cutoff of 300.0 eV were adopted. The convergence criterion for energy was the energy error of  $2.0 \times 10^{-6}$  eV/atom. Based on the optimized models, the band structure, the PDOS, and the electron density isosurfaces of the orbit (wavefunction) of  $\text{CH}_3\text{NH}_3\text{PbBr}_3$  and  $\text{CH}_3\text{NH}_3\text{PbBr}_3@\text{CsPbBr}_3$  were calculated.

The calculated band structure and PDOS are shown in Fig. S4. The energy gaps of  $\text{CH}_3\text{NH}_3\text{PbBr}_3$  and  $\text{CH}_3\text{NH}_3\text{PbBr}_3@\text{CsPbBr}_3$  are 2.37 and 2.41 eV, respectively. The

valence and the conduction bands are mainly consisted of Br<sup>-</sup> 2p, Pb<sup>2+</sup> 3p electronic state, respectively.

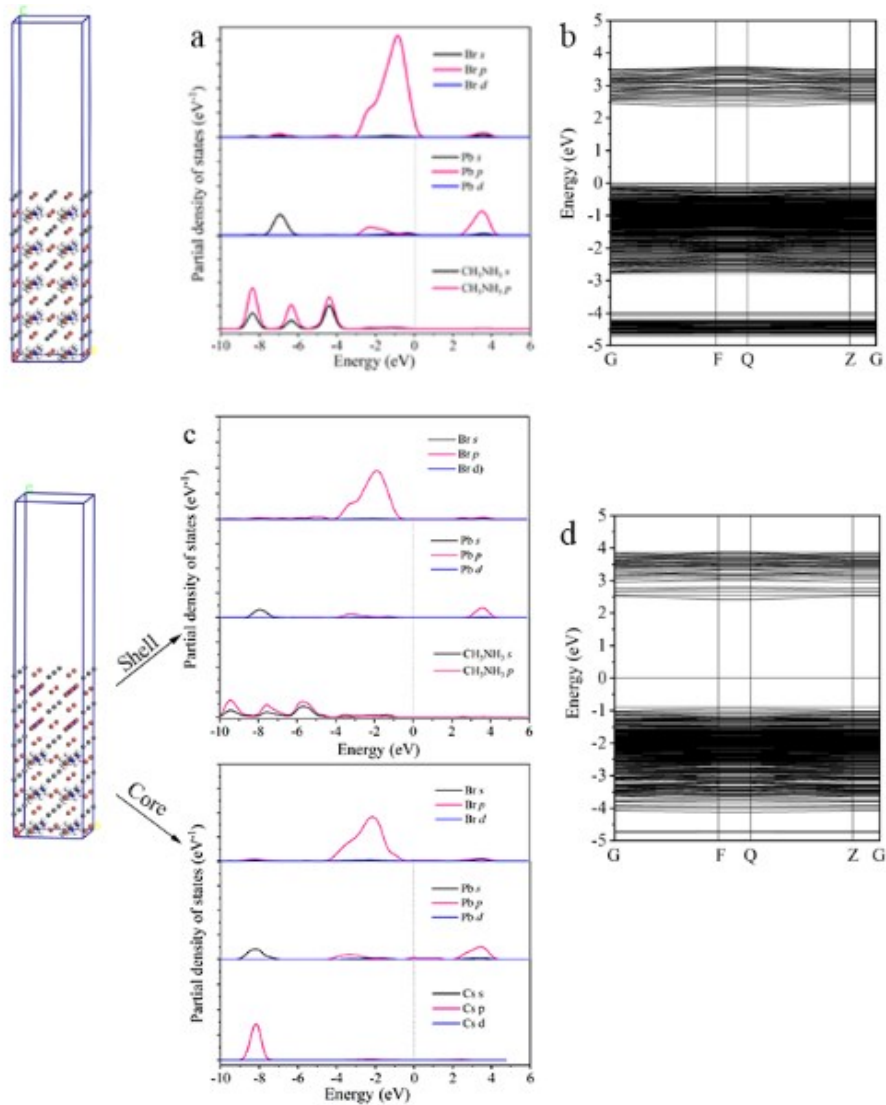


Fig. S4 PDOS (a) and band structure (b) for  $\text{CH}_3\text{NH}_3\text{PbBr}_3$ . PDOS of core and shell (c), band structure (d) for  $\text{CH}_3\text{NH}_3\text{PbBr}_3@ \text{CsPbBr}_3$

## 5. Instability

After QDs were placed in natural light, room temperature of about 25-35 °C and humidity of about 50-60% for more than four months, the XRD patterns of  $\text{CsPbBr}_3@ \text{CH}_3\text{NH}_3\text{PbBr}_3$  agree with those of the orthorhombic  $\text{PbBr}_2$  (JCPDS PDF#31-0679), as shown in Fig. 4a and Fig. S5, which confirms the formation of  $\text{PbBr}_2$ .

$\text{CH}_3\text{NH}_3\text{PbBr}_3$  may have decomposed into  $\text{CH}_3\text{NH}_3\text{Br}$  and  $\text{PbBr}_2$ , and  $\text{PbBr}_2$  emits a weak PL at about 400-500 nm. (*Chem. Commun.*, 2016, 52, 7118) Additionally, the organic shell of has been collapsed and decomposed, and the core has agglomerated. Thus the  $\text{CH}_3\text{NH}_3\text{PbBr}_3$  and  $\text{CsPbBr}_3@ \text{CH}_3\text{NH}_3\text{PbBr}_3$  QDs only have a weak PL at about 400-500 nm.

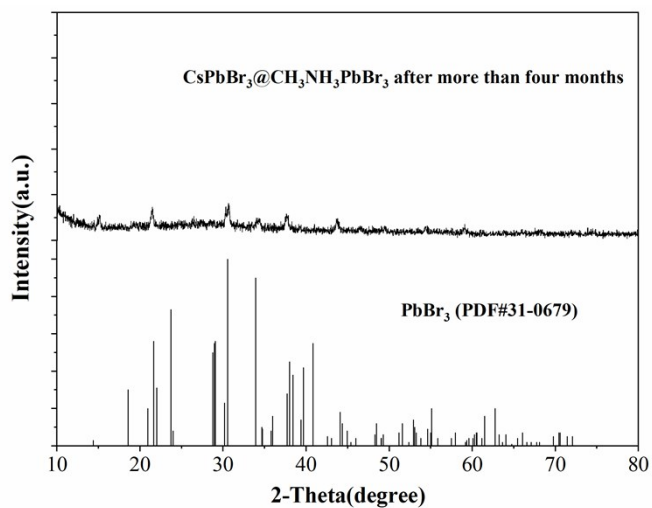


Fig. S5 XRD patterns of  $\text{CsPbBr}_3@ \text{CH}_3\text{NH}_3\text{PbBr}_3$  after more than four months and the orthorhombic  $\text{PbBr}_2$